JACS
JOURNAL OF THE AMERICAN CHEMICAL SOCIETY

pubs.acs.org/JACS

Communication

Self-Assembly and Ionic-Lattice-like Secondary Structure of a Flexible Linear Polymer of Highly Charged Inorganic Building Blocks

Guanyun Zhang, Eyal Gadot, Gal Gan-Or, Mark Baranov, Tal Tubul, Alevtina Neyman, Mu Li, Anna Clotet, Josep M. Poblet, Panchao Yin, and Ira A. Weinstock*

Cite This: J. Am. Chem. Soc. 2020, 142, 7295−7300

Read Online

ACCESS | Metrics & More | Article Recommendations | Supporting Information

ABSTRACT: Among molecular building blocks, metal oxide cluster anions and their countercations provide multiple options for the self-assembly of functional materials. Currently, however, rational design concepts are limited to electrostatic interactions with metal or organic countercations or to the attachment and subsequent reactions of functionalized organic ligands. We now demonstrate that bridging μ-oxo linkages can be used to string together a bifunctional Keggin anion building block, $[PNb_2Mo_{10}O_{40}]^{5-}$ (**1**), the diniobium(V) analogue of $[PV_2Mo_{10}O_{40}]^{5-}$ (**2**). Induction of μ-oxo ligation between the Nb^V=O moieties of **1** in acetonitrile via step-growth polymerization gives linear polymers with entirely inorganic backbones, some comprising over 140 000 repeating units, each with a 3− charge, exceeding that of previously reported organic or inorganic polyelectrolytes. As the chain grows, its flexible μ-oxo-linked backbone, with associated countercations, coils into a compact 270 nm diameter spherical secondary structure as a result of electrostatic interactions not unlike those within ionic lattices. More generally, the findings point to new options for the rational design of multidimensional structures based on μ-oxo linkages between Nb^V=O-functionalized building blocks.

Soluble components are routinely utilized as structural building units (SBUs) for the self-assembly of functional materials.[1−5] In this context, metal oxide cluster anions, or polyoxometalates (POMs), are used as SBUs for assemblies featuring the extensive and readily tunable electronic and catalytic properties of the POM building blocks themselves.[6−13] The challenge in these efforts generally is to develop methods based on rational design principles, which in turn requires detailed understanding of how interactions in solution lead to specific hierarchical organizations.[14]

In this regard, POMs and their countercations provide inherent opportunities for utilizing electrostatic interactions as a driving force for self-assembly. For this, alkali-metal,[15] transition-metal,[16] organic,[17] or metallo-organic cations[9] can be introduced, and the structural outcomes are often thermodynamically controlled. Examples include the use of alkali-metal cations to generate hollow single-walled vesicles[18,19] and the use of large organic cations to generate amphiphilic building blocks.[17] Moreover, by grafting of polyfunctional organic tethers to the POM itself, the introduction of transition-metal cations can lead to open-framework structures[20] or low-nuclearity molecular units that spontaneously self-assemble into large supramolecular structures.[21,22] Related methods have led to POM−conductive polymer composites,[23] precisely defined oligomeric structures,[24,25] and organic−inorganic polymers.[26]

We now demonstrate the formation of μ-oxo linkages[25] between a suitably designed bifunctional Keggin anion building block, $[PNb_2Mo_{10}O_{40}]^{5-}$ (**1**), the diniobium(V) analogue of the well-known divanadium complex $[PV_2Mo_{10}O_{40}]^{5-}$ (**2**).[27] Upon μ-oxo linkage formation in acetonitrile, **1** serves as the repeating unit in an entirely inorganic analogue of organic polyethers (Figure 1). The linear polymer's inorganic backbone grows to more than 140 000 POM units (252 MDa), a

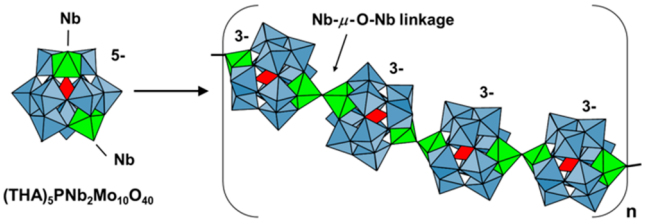

Figure 1. Formation of a polyether-like inorganic polymer from the bifunctional Keggin anion α-$[PNb_2Mo_{10}O_{40}]^{5-}$ (**1**) (red, P-centered tetrahedra; blue, Mo-centered polyhedra; green, Nb-centered polyhedra). Each linked **1** unit possesses a 3− charge.

degree of polymerization (DP) approximately 60% that of 1 MDa poly(ethylene glycol) (PEG).[28] Moreover, each linked POM has a 3− charge, exceeding that of repeating units in any known organic or inorganic polyelectrolyte.[29]

Linear growth of these flexible chains, documented by dynamic light scattering (DLS), small-angle X-ray scattering (SAXS), and cryogenic transmission electron microscopy (cryo-TEM), leads to tightly coiled soluble spheres, as large

Received: February 7, 2020
Published: April 1, 2020

https://dx.doi.org/10.1021/jacs.0c01486
J. Am. Chem. Soc. 2020, 142, 7295−7300

as 270 nm in diameter. Their compact secondary structure is fully understood as a natural extension of established models for the coiling of much less highly charged polyelectrolytes.[30,31] Moreover, the methodology presented here points to new options for the assembly of higher-dimensional structures via ether-like μ-oxo linkages between entirely inorganic building blocks.

While terminal V^V=O ligands at the surface of **2** and other POMs are inert, POM-complexed Nb^V=O moieties readily form μ-oxo linkages via acid condensation, as in the conversion of 2 equiv of A-α-$[SiNb_3W_9O_{40}]^{7-}$ to A-α-$[Si_2Nb_6W_{18}O_{77}]^{8-}$ (eq 1).[32−35] Accordingly, the incorporation of two Nb^V=O

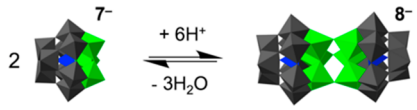

(1)

moieties distal to one another as in **1** should give bifunctional units that polymerize into linear chains (Figure 1). The anions **1** were prepared by adding Na_2HPO_4, Na_2MoO_4, and acid to $K_8Nb_6O_{19}$ in aqueous H_2O_2.[36] After workup, yellow needlelike crystals of $K_5[PNb_2Mo_{10}O_{40}]$ (K_5**1**) were isolated in 42% yield (Figures S1 and S2). The ^{31}P NMR spectrum of **1** contains multiple overlapping signals (Figure 2, upper right inset) that, by analogy to **2** (Figure S3),[37] are attributed to five positional isomers of the two Nb atoms.

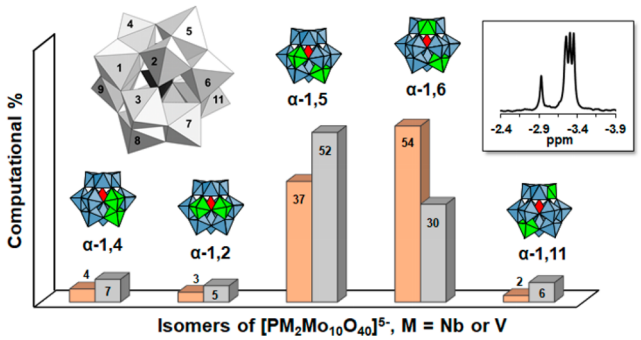

Figure 2. Theoretical distributions of five isomers of $[PM_2Mo_{10}O_{40}]^{5-}$ (red, P; blue, Mo; green, Nb or V) for **2** (orange bars) and **1** (gray bars). The left inset shows the key to addendum atom positions. The right inset shows the ^{31}P NMR spectrum of K_5**1** in D_2O.

To further validate this, DFT methods[38,39] were used to calculate relative energies and abundances of the positional isomers of **1** and **2** (Figure 2 and Table S1). Not only were five stable isomers of **1** identified, but the Nb=O moieties in three of them, α-1,5, α-1,6, and α-1,11—constituting 88% of those present—are distal to one another and suitable for serving as linkages in linear chains. As in **2**, the positional isomers of **1** are in dynamic equilibrium, with changes in their relative ^{31}P NMR intensities observed as functions of pH. For **1**, this potentially allows for dynamic replenishment of distal-functionalized isomers consumed during polymerization.

Next, K_5**1** was extracted into a CH_2Cl_2 solution of tetrahexylammonium bromide (THABr), from which waxy-yellow THA_5**1** was isolated (Figures 3A and S4−S6). Electrospray ionization mass spectrometry (ESI-MS) gave an envelope of signals matching the 1+ ion, $\{(THA)_5H[PNb_2Mo_{10}O_{40}]\}^+$ (Figure 3B). After several months at 4 °C, a solution of THA_5**1** (0.1 g) in 1 mL of tetrahydrofuran

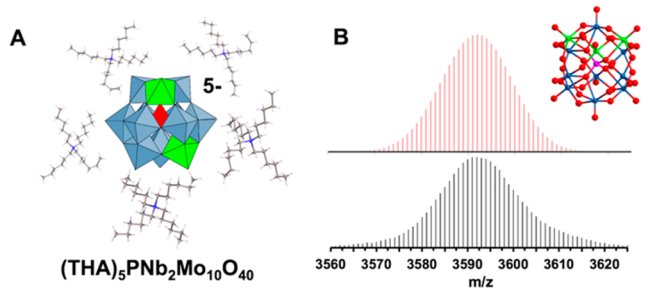

Figure 3. (A) The α-1,6-**1** cluster and its five THA countercations. (B) ESI-MS spectra of THA_5**1** in MeCN with experimental (black) and simulated (red) isotopic envelopes corresponding to $\{(THA)_5H1\}^+$. The inset shows a ball-and-stick model of crystallographically determined α-1,4-**1** (blue, Mo; green, disordered Nb; purple, P; red, O).

delivered yellow crystals. Data from single-crystal X-ray diffraction identified the α-1,4 isomer of **1**, with two corner-shared Nb atoms (Figure 3B inset; disorder gave partial occupancies at three positions: Figures S7−S9 and Tables S2−S5).

Polymerization of THA_5**1** in MeCN was induced by addition of 25 equiv of 30% aqueous H_2O_2 under air. ^{31}P NMR spectra obtained every 24 h revealed new signals, with slow loss of those assigned to **1** (Figure S10). After 72 h, the ^{31}P NMR spectrum was entirely different. In addition, the FTIR spectrum of a dried sample featured a new band at 671 cm^{-1}, diagnostic for intermolecular Nb−O−Nb linkages between POM anions (Figure S11),[32,34,35] and large objects were observed by DLS (Figure 4A) and SAXS (Figure 4B).

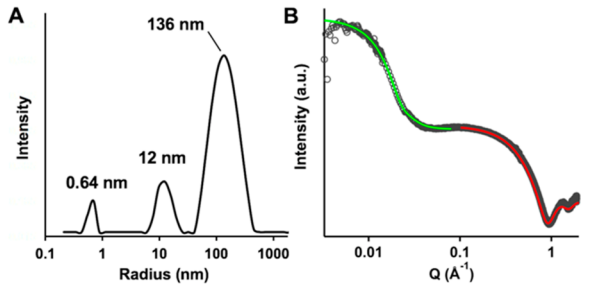

Figure 4. (A) Hydrodynamic radii (as determined by DLS) after polymerization of **1** in MeCN. (B) SAXS data (the y axis is logarithmic) for a concentrated sample of the solution (gray circles), and fitted curves of compact solid spheres (green) and Keggin-type POMs (red).

The smallest size domain observed by DLS, with R = 0.64 nm, is due to the presence of monomeric **1**, while larger structures were observed with average hydrodynamic radii of 12 and 136 nm. Because of the sixth-order dependence of the scattering intensity on the radius, the more abundant smaller objects, monomeric **1** and medium-sized objects, were more dominant in SAXS analysis (Figure 4B), which revealed two distinct regions. Fitting of the q < 0.1 $Å^{-1}$ region indicated the presence of compact spheres with an average radius of ca. 15 nm. The compact nature of the coiled polymers was further confirmed by DLS and static light scattering (SLS) (Figure S12). Scattering at q > 0.1 $Å^{-1}$ confirmed the presence of individual, freely diffusing Keggin anions. After more than a month in solution, the same size domains were observed with identical relative intensities.

https://dx.doi.org/10.1021/jacs.0c01486
J. Am. Chem. Soc. 2020, 142, 7295−7300

Polymerization of **1** in MeCN in the presence of aqueous H_2O_2 and air was then investigated. Notably, air plays an important role: when THA_5**1** was treated with H_2O_2 under argon, no reaction occurred (Figure S13 and Table S6). This suggested that under air, the acid required for polymerization was supplied by steady conversion of CO_2 to carbonic acid in the wet mixture of MeCN and aqueous H_2O_2. Consistent with this, polymerization indeed occurred under pure CO_2 (Figures S13 and S14), and the reaction mixture was found by ESI-MS to contain THA salts of HCO_3^- and CO_3^{2-} (Figure S15). Moreover, while acid alone gave no reaction, treatment of THA_5**1** with excess acetic acid and H_2O_2 gave the orange diperoxo complex $(THA)_5P(NbO_2)_2Mo_{10}O_{38}$ (THA_5**3**) in 83% yield (Figures S16–S19).

These results suggest an acid-concentration-controlled balance between peroxidation and polymerization and a catalytic role for H_2O_2[32] during polymerization. Namely, peroxide-ligated Nb(V) atoms react with acid to give μ-O linkages,[33] with the requisite H^+ supplied by steady dissolution of CO_2 from the air (Figure 5). Consistent with this, when **3**

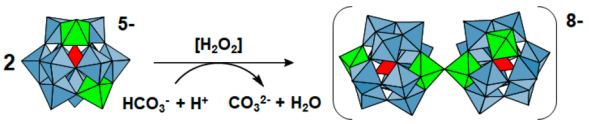

Figure 5. Peroxide-catalyzed acid condensation of Nb^V=O moieties of **1** in wet MeCN under air.

was reacted with 1 equiv of **1** under air—*with no added* H_2O_2—polymerization occurred in 1 day, 3 times faster than when **1** was treated with H_2O_2 (Figures S20 and S21). Finally, this mechanism should lead to step-growth polymerization, typified by equilibrated mixtures of unreacted monomers and polymers with variable DP values.[40,41]

This was indeed observed in cryo-TEM images obtained after polymerization, which revealed individual monomeric units (Figure 6A), flexible linear chains in the early stages of coiling (Figure 6B), small coiled chains (Figure 6C), and large, tightly coiled spherical polymers (Figures 6D and S22). On the basis of statistical analysis of particle sizes and interparticle distances (Figure S23), the minimum estimated DP of an average-sized tightly coiled 270 nm diameter sphere is 140 000 repeating units, with a total negative charge of 420 000− counterbalanced by an equal number of THA cations. The mass of the inorganic backbone alone is 252 MDa.

This tendency to coil into compact structures is consistent with the documented behavior of flexible-chain polyelectrolytes. For rigid polyelectrolytes,[42] charge repulsion is attenuated by the presence of countercations in the vicinity of the polymer surface. The net charges of the particles and their double layers lead to repulsive interactions that prevent aggregation. For flexible polyelectrolytes, however, repeating unit charges and associated counterions cause the polymer to shrink to a volume much less than that of a statistical coil "as a consequence of intramolecular electrostatic attraction of the sort which stabilizes an ionic lattice".[31] For organic and inorganic polyelectrolytes, monomer unit charges greater than unity are rare.[26] In the present case, with tens of thousands of closely spaced 3− units, the formation of tightly coiled structures is readily understood. Moreover, because the high charges and large DP values, the polymers remain tightly coiled even after exchanging THA for tetramethylammonium cation

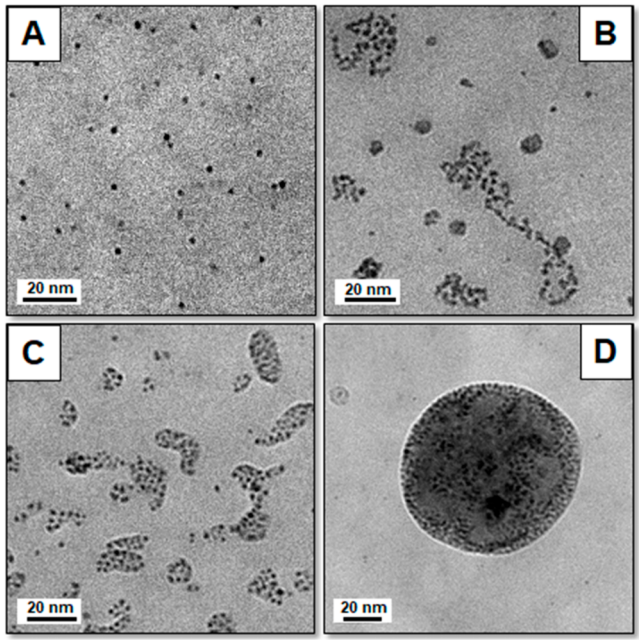

Figure 6. Cryo-TEM images after polymerization of THA_5**1** under air in MeCN: (A) monomeric units; (B) linear oligomeric chains; (C) small coiled polymers; (D) a tightly coiled ca. 100 nm diameter spherical polymer.

(TMA) or Li^+ and dissolution of the resultant structures in water (Figures S24–S29).

Finally, the presence of intact molecules of **1** in the polymerized structures was supported by FTIR spectroscopy; only slight changes were observed (Figure S11). Even more definitive confirmation was obtained by cleaving the polymeric structures to individual Keggin ion derivatives. As noted above, excess H_2O_2 and glacial acetic acid cleanly convert **1** to the orange diperoxo derivative **3**, whose ^{31}P NMR spectrum is shown at the upper right in Figure 7A. Addition of those reagents to polymeric **1** led to a color change from pale to dark orange (Figure S30), and only individual monomer units were observed by DLS (Figure S31). The solution now contained **3**, with its characteristic ^{31}P NMR spectrum (bottom right in Figure 7A; see Figure S32 for the ESI-MS spectrum). Moreover, only individual Keggin anions were observed by cryo-TEM (Figure 7B).

The formation of μ-oxo-linked polymers is not limited to polyoxomolybdates. This was shown by the preparation of $THA_8P_2Nb_2W_{16}O_{62}$, the THA salt of a bis(Nb^V=O) derivative of the plenary Wells–Dawson anion (Figures S33–S37). When this was treated with H_2O_2 in MeCN under air, large objects were observed by DLS after several days, and TEM images consistent with large coiled polymers were obtained (Figures S38–S40). Moreover, after treatment with excess H_2O_2 and glacial acetic acid, only individual monomeric units were observed by DLS and cryo-TEM, and ^{31}P NMR and ESI-MS spectra were diagnostic for the diperoxo derivative (Figures S41 and S42).

In summary, the versatile reactivity of terminal oxo ligands of Nb^V=O addendum atoms in heteropoly molybdates (**1**) and tungstates is shown to provide access to μ-oxo linkages between highly charged inorganic building blocks. Stepwise growth of these flexible chains, documented by DLS, SAXS, and cryo-TEM, leads to soluble compact spheres with

https://dx.doi.org/10.1021/jacs.0c01486
J. Am. Chem. Soc. 2020, 142, 7295–7300

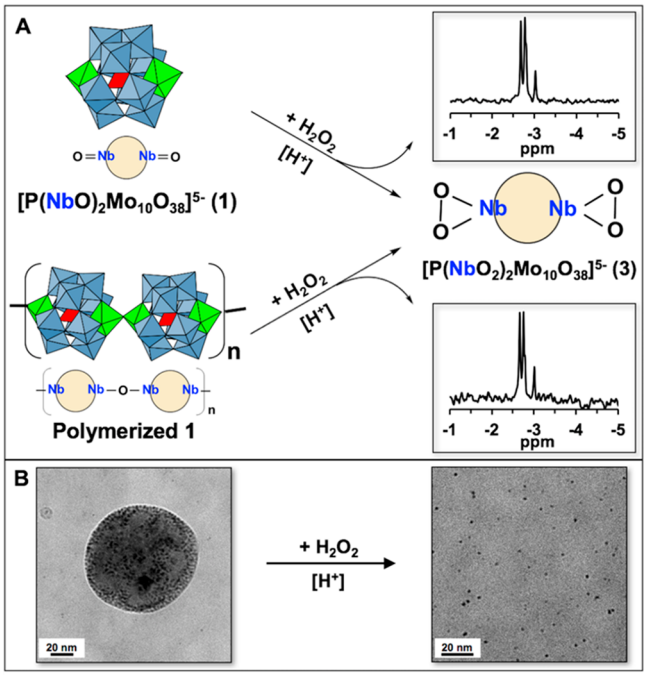

Figure 7. (A) Conversion of **1** (upper left) and polymeric **1** (lower left) to diperoxo derivative **3** (center right) by addition of acid and H_2O_2. The insets at the upper and lower right are the corresponding ^{31}P NMR spectra. (B) Cryo-TEM images before and after conversion of polymeric **1** to individual derivative **3** by addition of acid and H_2O_2.

diameters of up to 270 nm whose tightly coiled secondary structures are consistent with ionic-lattice-like electrostatic interactions inherent to the stabilization of flexible polyelectrolytes in solution.[30,31] These interactions, originally found for polymers with singly charged repeating units,[43,44] are inevitably dominant for linear chains derived from building blocks such as **1**, which are more highly charged than any discussed in nearly a century of polyelectrolyte theory. More generally, the methodology presented here points to new options for the assembly of functional higher-dimensional structures via the formation of ether-like μ-oxo linkages between Nb^V=O-functionalized building blocks.

■ ASSOCIATED CONTENT

Supporting Information

The Supporting Information is available free of charge at https://pubs.acs.org/doi/10.1021/jacs.0c01486.

Crystallographic data for $[PNb_2Mo_{10}O_{40}]^{5-}$ (CIF)
DFT calculations, spectroscopic data, and cryo-TEM images (PDF)

■ AUTHOR INFORMATION

Corresponding Author

Ira A. Weinstock − *Department of Chemistry and the Ilse Katz Institute for Nanoscale Science & Technology, Ben-Gurion University of the Negev, Beer Sheva 84105, Israel;* orcid.org/0000-0002-6701-2001; Email: iraw@bgu.ac.il

Authors

Guanyun Zhang − *Department of Chemistry and the Ilse Katz Institute for Nanoscale Science & Technology, Ben-Gurion University of the Negev, Beer Sheva 84105, Israel*

Eyal Gadot − *Department of Chemistry and the Ilse Katz Institute for Nanoscale Science & Technology, Ben-Gurion University of the Negev, Beer Sheva 84105, Israel*

Gal Gan-Or − *Department of Chemistry and the Ilse Katz Institute for Nanoscale Science & Technology, Ben-Gurion University of the Negev, Beer Sheva 84105, Israel*

Mark Baranov − *Department of Chemistry and the Ilse Katz Institute for Nanoscale Science & Technology, Ben-Gurion University of the Negev, Beer Sheva 84105, Israel*

Tal Tubul − *Department of Chemistry and the Ilse Katz Institute for Nanoscale Science & Technology, Ben-Gurion University of the Negev, Beer Sheva 84105, Israel*

Alevtina Neyman − *Department of Chemistry and the Ilse Katz Institute for Nanoscale Science & Technology, Ben-Gurion University of the Negev, Beer Sheva 84105, Israel*

Mu Li − *South China Advanced Institute for Soft Matter Science and Technology & State Key Laboratory of Luminescent Materials and Devices, South China University of Technology, Guangzhou 510640, China*

Anna Clotet − *Departament de Química Física i Inorgànica, Universitat Rovira i Virgili, E-43007 Tarragona, Spain;* orcid.org/0000-0003-0543-6607

Josep M. Poblet − *Departament de Química Física i Inorgànica, Universitat Rovira i Virgili, E-43007 Tarragona, Spain;* orcid.org/0000-0002-4533-0623

Panchao Yin − *South China Advanced Institute for Soft Matter Science and Technology & State Key Laboratory of Luminescent Materials and Devices, South China University of Technology, Guangzhou 510640, China;* orcid.org/0000-0003-2902-8376

Complete contact information is available at: https://pubs.acs.org/10.1021/jacs.0c01486

Author Contributions

G.Z. and E.G. contributed equally.

Notes

The authors declare no competing financial interest.

■ ACKNOWLEDGMENTS

I.A.W. thanks the Israel Science Foundation (ISF) (170/17). I.A.W. and P.Y. thank the National Natural Science Foundation of China−ISF Joint Grant Program (3102/19). G.Z. thanks PBC-Israel for a fellowship. This project was also supported by the Spanish Ministerio de Ciencia e Innovación (CTQ2017-87269-P) and the Generalitat de Catalunya (2014SGR199). J.M.P. also thanks the ICREA Foundation for an ICREA ACADEMIA Award.

■ REFERENCES

(1) Wang, Q.; Astruc, D. State of the Art and Prospects in Metal−Organic Framework (MOF)-Based and MOF-Derived Nanocatalysis. *Chem. Rev.* **2020**, *120*, 1438.

(2) Boles, M. A.; Engel, M.; Talapin, D. V. Self-Assembly of Colloidal Nanocrystals: From Intricate Structures to Functional Materials. *Chem. Rev.* **2016**, *116*, 11220−11289.

(3) Schoedel, A.; Li, M.; Li, D.; O'Keeffe, M.; Yaghi, O. M. Structures of Metal−Organic Frameworks with Rod Secondary Building Units. *Chem. Rev.* **2016**, *116*, 12466−12535.

(4) Cook, T. R.; Zheng, Y.-R.; Stang, P. J. Metal−Organic Frameworks and Self-Assembled Supramolecular Coordination Complexes: Comparing and Contrasting the Design, Synthesis, and Functionality of Metal−Organic Materials. *Chem. Rev.* **2013**, *113*, 734−777.

(5) Llordes, A.; Garcia, G.; Gazquez, J.; Milliron, D. J. Tunable Near-Infrared and Visible-Light Transmittance in Nanocrystal-in-Glass Composites. *Nature* **2013**, *500*, 323−326.
(6) Anyushin, A. V.; Kondinski, A.; Parac-Vogt, T. N. Hybrid Polyoxometalates as Post-Functionalization Platforms: From Fundamentals to Emerging Applications. *Chem. Soc. Rev.* **2020**, *49*, 382−432.
(7) Chen, L.; San, K. A.; Turo, M. J.; Gembicky, M.; Fereidouni, S.; Kalaj, M.; Schimpf, A. M. Tunable Metal Oxide Frameworks via Coordination Assembly of Preyssler-Type Molecular Clusters. *J. Am. Chem. Soc.* **2019**, *141*, 20261−20268.
(8) Hampson, E.; Cameron, J. M.; Amin, S.; Kyo, J.; Watts, J. A.; Oshio, H.; Newton, G. N. Asymmetric Hybrid Polyoxometalates: A Platform for Multifunctional Redox-Active Nanomaterials. *Angew. Chem., Int. Ed.* **2019**, *58*, 18281−18285.
(9) Stuckart, M.; Monakhov, K. Y. Polyoxometalates as Components of Supramolecular Assemblies. *Chem. Sci.* **2019**, *10*, 4364−4376.
(10) Qin, J.-S.; Du, D.-Y.; Guan, W.; Bo, X.-J.; Li, Y.-F.; Guo, L.-P.; Su, Z.-M.; Wang, Y.-Y.; Lan, Y.-Q.; Zhou, H.-C. Ultrastable Polymolybdate-Based Metal−Organic Frameworks as Highly Active Electrocatalysts for Hydrogen Generation from Water. *J. Am. Chem. Soc.* **2015**, *137*, 7169−7177.
(11) Zhao, C.; Glass, E. N.; Chica, B.; Musaev, D. G.; Sumliner, J. M.; Dyer, R. B.; Lian, T.; Hill, C. L. All-Inorganic Networks and Tetramer Based on Tin(II)-Containing Polyoxometalates: Tuning Structural and Spectral Properties with Lone-Pairs. *J. Am. Chem. Soc.* **2014**, *136*, 12085−12091.
(12) Proust, A.; Matt, B.; Villanneau, R.; Guillemot, G.; Gouzerh, P.; Izzet, G. Functionalization and Post-Functionalization: A Step Towards Polyoxometalate-Based Materials. *Chem. Soc. Rev.* **2012**, *41*, 7605−7622.
(13) Dolbecq, A.; Dumas, E.; Mayer, C. R.; Mialane, P. Hybrid Organic−Inorganic Polyoxometalate Compounds: From Structural Diversity to Applications. *Chem. Rev.* **2010**, *110*, 6009−6048.
(14) Kulikov, V.; Johnson, N. A. B.; Surman, A. J.; Hutin, M.; Kelly, S. M.; Hezwani, M.; Long, D.-L.; Meyer, G.; Cronin, L. Spontaneous Assembly of an Organic−Inorganic Nucleic Acid Z-DNA Double-Helix Structure. *Angew. Chem., Int. Ed.* **2017**, *56*, 1141−1145.
(15) (a) Misra, A.; Kozma, K.; Streb, C.; Nyman, M. Beyond Charge Balance: Counter-Cations in Polyoxometalate Chemistry. *Angew. Chem., Int. Ed.* **2020**, *59*, 596−612. (b) Soltis, J. A.; Wallace, C. M.; Penn, R. L.; Burns, P. C. Cation-Dependent Hierarchical Assembly of U60 Nanoclusters into Macro-Ion Assemblies Imaged via Cryogenic Transmission Electron Microscopy. *J. Am. Chem. Soc.* **2016**, *138*, 191−198.
(16) Turo, M. J.; Chen, L.; Moore, C. E.; Schimpf, A. M. Co^{2+}-Linked $[NaP_5W_{30}O_{110}]^{14-}$: A Redox-Active Metal Oxide Framework with High Electron Density. *J. Am. Chem. Soc.* **2019**, *141*, 4553−4557.
(17) Li, B.; Li, W.; Li, H.; Wu, L. Ionic Complexes of Metal Oxide Clusters for Versatile Self-Assemblies. *Acc. Chem. Res.* **2017**, *50*, 1391−1399.
(18) Yin, P.; Li, D.; Liu, T. Solution Behaviors and Self-Assembly of Polyoxometalates as Models of Macroions and Amphiphilic Polyoxometalate−Organic Hybrids as Novel Surfactants. *Chem. Soc. Rev.* **2012**, *41*, 7368−7383.
(19) Liu, T.; Langston, M. L. K.; Li, D.; Pigga, J. M.; Pichon, C.; Todea, A. M.; Müller, A. Self-Recognition Among Different Polyprotic Macroions During Assembly Processes in Dilute Solution. *Science* **2011**, *331*, 1590−1592.
(20) Li, X.-X.; Zhao, D.; Zheng, S.-T. Recent Advances in POM-Organic Frameworks and POM-Organic Polyhedra. *Coord. Chem. Rev.* **2019**, *397*, 220−240.
(21) Piot, M.; Abécassis, B.; Brouri, D.; Troufflard, C.; Proust, A.; Izzet, G. Control of the Hierarchical Self-Assembly of Polyoxometalate-Based Metallomacrocycles by Redox Trigger and Solvent Composition. *Proc. Natl. Acad. Sci. U. S. A.* **2018**, *115*, 8895−8900.
(22) Izzet, G.; Abécassis, B.; Brouri, D.; Piot, M.; Matt, B.; Serapian, S. A.; Bo, C.; Proust, A. Hierarchical Self-Assembly of Polyoxometalate-Based Hybrids Driven by Metal Coordination and Electrostatic Interactions: From Discrete Supramolecular Species to Dense Monodisperse Nanoparticles. *J. Am. Chem. Soc.* **2016**, *138*, 5093−5099.
(23) Herrmann, S.; Ritchie, C.; Streb, C. Polyoxometalate − Conductive Polymer Composites for Energy Conversion, Energy Storage and Nanostructured Sensors. *Dalton Trans.* **2015**, *44*, 7092−7104.
(24) Macdonell, A.; Johnson, N. A. B.; Surman, A. J.; Cronin, L. Configurable Nanosized Metal Oxide Oligomers via Precise "Click" Coupling Control of Hybrid Polyoxometalates. *J. Am. Chem. Soc.* **2015**, *137*, 5662−5665.
(25) (a) Schwarz, B.; Dürr, M.; Kastner, K.; Heber, N.; Ivanović-Burmazović, I.; Streb, C. Solvent-Controlled Polymerization of Molecular Strontium Vanadate Monomers into 1D Strontium Vanadium Oxide Chains. *Inorg. Chem.* **2019**, *58*, 11684−11688. (b) Hou, Y.; Zakharov, L. N.; Nyman, M. Observing Assembly of Complex Inorganic Materials from Polyoxometalate Building Blocks. *J. Am. Chem. Soc.* **2013**, *135*, 16651−16657.
(26) Guan, W.; Wang, G.; Ding, J.; Li, B.; Wu, L. A Supramolecular Approach of Modified Polyoxometalate Polymerization and Visualization of a Single Polymer Chain. *Chem. Commun.* **2019**, *55*, 10788−10791.
(27) Weinstock, I. A.; Schreiber, R. E.; Neumann, R. Dioxygen in Polyoxometalate Mediated Reactions. *Chem. Rev.* **2018**, *118*, 2680−2717.
(28) Banasik, B.; Nadala, C.; Samadpour, M. An Economical and Scalable Preparation of Poly(Ethylene Glycol) Methyl Ether Amine, M.W. 5,000. *Org. Prep. Proced. Int.* **2018**, *50*, 95−99.
(29) Raffa, P.; Wever, D. A. Z.; Picchioni, F.; Broekhuis, A. A. Polymeric Surfactants: Synthesis, Properties, and Links to Applications. *Chem. Rev.* **2015**, *115*, 8504−8563.
(30) Dintzis, H. M.; Oncley, J. L.; Fuoss, R. M. Dielectric Increments in Aqueous Solutions of Synthetic Polyelectrolytes. *Proc. Natl. Acad. Sci. U. S. A.* **1954**, *40*, 62−70.
(31) Fuoss, R. M. Polyelectrolytes. *Discuss. Faraday Soc.* **1951**, *11*, 125−134.
(32) Maksimchuk, N. V.; Maksimov, G. M.; Evtushok, V. Y.; Ivanchikova, I. D.; Chesalov, Y. A.; Maksimovskaya, R. I.; Kholdeeva, O. A.; Solé-Daura, A.; Poblet, J. M.; Carbó, J. J. Relevance of Protons in Heterolytic Activation of H_2O_2 over Nb(V): Insights from Model Studies on Nb-Substituted Polyoxometalates. *ACS Catal.* **2018**, *8*, 9722−9737.
(33) Li, S.-J.; Liu, S.-X.; Li, C.-C.; Ma, F.-J.; Liang, D.-D.; Zhang, W.; Tan, R.-K.; Zhang, Y.-Y.; Xu, L. Reactivity of Polyoxoniobates in Acidic Solution: Controllable Assembly and Disassembly Based on Niobium-Substituted Germanotungstates. *Chem. - Eur. J.* **2010**, *16*, 13435−13442.
(34) Kim, G.-S.; Zeng, H.; Neiwert, W. A.; Cowan, J. J.; VanDerveer, D.; Hill, C. L.; Weinstock, I. A. Dimerization of A-α-$[SiNb_3W_9O_{40}]^{7-}$ by pH-Controlled Formation of Individual Nb−μ-O−Nb Linkages. *Inorg. Chem.* **2003**, *42*, 5537−5544.
(35) Finke, R. G.; Droege, M. W. Trisubstituted Heteropolytungstates as Soluble Metal Oxide Analogs. 1. The Preparation, Characterization, and Reactions of Organic Solvent Soluble Forms of $Si_2W_{18}Nb_6O_{77}^{8-}$, $SiW_9Nb_3O_{40}^{7-}$, and the $SiW_9Nb_3O_{40}^{7-}$ Supported Organometallic Complex $[(C_5Me_5)Rh{\cdot}SiW_9Nb_3O_{40}]^{5-}$. *J. Am. Chem. Soc.* **1984**, *106*, 7274−7277.
(36) Abramov, P. A.; Shmakova, A. A.; Haouas, M.; Fink, G.; Cadot, E.; Sokolov, M. N. Self-Assembly of $[PNb_xW_{12-x}O_{40}]^{n-}$ Keggin Anions − a Simple Way to Mixed Nb−W Polyoxometalates. *New J. Chem.* **2017**, *41*, 256−262.
(37) Pettersson, L.; Andersson, I.; Grate, J. H.; Selling, A. Multicomponent Polyanions. 46. Characterization of the Isomeric Keggin Decamolybdodivanadophosphate Ions in Aqueous Solution by ^{31}P and ^{51}V NMR. *Inorg. Chem.* **1994**, *33*, 982−993.
(38) Prabhakaran, V.; Lang, Z.; Clotet, A.; Poblet, J. M.; Johnson, G. E.; Laskin, J. Controlling the Activity and Stability of Electrochemical Interfaces Using Atom-by-Atom Metal Substitution of Redox Species. *ACS Nano* **2019**, *13*, 458−466.

https://dx.doi.org/10.1021/jacs.0c01486
J. Am. Chem. Soc. 2020, 142, 7295−7300

(39) Yan, L.; López, X.; Carbó, J. J.; Sniatynsky, R.; Duncan, D. C.; Poblet, J. M. On the Origin of Alternating Bond Distortions and the Emergence of Chirality in Polyoxometalate Anions. *J. Am. Chem. Soc.* **2008**, *130* (26), 8223−8233.
(40) Koltzenburg, S.; Maskos, M.; Nuyken, O. Step-Growth Polymerization. In *Polymer Chemistry*; Springer: Berlin, 2017; pp 163−204.
(41) Liu, K.; Nie, Z.; Zhao, N.; Li, W.; Rubinstein, M.; Kumacheva, E. Step-Growth Polymerization of Inorganic Nanoparticles. *Science* **2010**, *329*, 197−200.
(42) Zhang, Z.; Murayama, T.; Sadakane, M.; Ariga, H.; Yasuda, N.; Sakaguchi, N.; Asakura, K.; Ueda, W. Ultrathin Inorganic Molecular Nanowire Based on Polyoxometalates. *Nat. Commun.* **2015**, *6*, 7731.
(43) Edelson, D.; Fuoss, R. M. A Contrast between Polyelectrolytes and Simple Electrolytes. *J. Am. Chem. Soc.* **1950**, *72*, 306−310.
(44) Edelson, D.; Fuoss, R. M. Chain Electrolytes. *J. Am. Chem. Soc.* **1948**, *70*, 2832.

https://dx.doi.org/10.1021/jacs.0c01486
J. Am. Chem. Soc. 2020, 142, 7295−7300